

Article

Investigation of the Tribological Properties of Hybrid Additive-Modified Water-Based Lubricating Fluid

Raimondas Kreivaitis , Jolanta Treinytė, Artūras Kupčinskas, Milda Gumbytė and Eglė Sendžikienė * 

Agriculture Academy, Vytautas Magnus University, K. Donelaičio str. 58, 44248 Kaunas, Lithuania

* Correspondence: egle.sendzikiene@vdu.lt; Tel.: +370-37-75-22-92

Abstract: Water-based lubricating fluids (WBLFs), known for their significant environmental benefits, are the focus of this study. The properties of WBLFs directly influence lubricated mechanisms' longevity and operating efficiency. WBLFs are enhanced using additives, which must improve their properties and, at the same time, remain environmentally friendly. This study combines bis(2-hydroxyethyl) ammonium erucate protic ionic liquid and titanium oxide nanoparticles to formulate the hybrid additive. The lubricity was investigated using Alumina/Bearing steel and WC/Bearing steel friction pairs in a reciprocating ball-on-plate tribo-tester. The results show that protic ionic liquid can significantly improve lubricity and the corrosion-preventing ability of the base fluid. Applying a hybrid additive further improved the wear reduction ability in the WC/Bearing steel friction pair. However, the wear reduction ability was diminished when a hybrid additive was used to lubricate the Alumina/Bearing steel friction pair. The proposed lubricity improvement mechanism is based on forming an adsorption layer of ionic liquid molecules and rolling and tribo-sintering titanium oxide nanoparticles.

Keywords: lubrication; protic ionic liquid; nanoparticles; hybrid additives; glycerol; aqueous; friction; wear



Citation: Kreivaitis, R.; Treinytė, J.; Kupčinskas, A.; Gumbytė, M.; Sendžikienė, E. Investigation of the Tribological Properties of Hybrid Additive-Modified Water-Based Lubricating Fluid. *Lubricants* **2024**, *12*, 178. <https://doi.org/10.3390/lubricants12050178>

Received: 19 March 2024

Revised: 8 May 2024

Accepted: 13 May 2024

Published: 15 May 2024



Copyright: © 2024 by the authors. Licensee MDPI, Basel, Switzerland. This article is an open access article distributed under the terms and conditions of the Creative Commons Attribution (CC BY) license (<https://creativecommons.org/licenses/by/4.0/>).

1. Introduction

Water-based lubricating fluids (WBLFs) are widely utilized in industrial, manufacturing, and automotive applications. An immense amount of WBLF is used worldwide. According to market reports, water-based metalworking fluids alone comprised $1.14 \times 10^6 \text{ m}^3$ annually [1]. WBLFs are used to lubricate moving parts in ships, hydropower plants, and dams to reduce the environmental impact in the case of leaks or accidents. The properties such as lubricity, cooling capacity, and rust prevention ability are critical in any of these applications. Water alone possesses poor performance. Therefore, it must be improved to meet the requirements of particular applications. WBLFs are formulated with various additives to enhance their lubricity and corrosion inhibition, protecting against microbial growth, maintaining pH and viscosity, and reducing foaming [2–4]. The additives are carefully selected and blended to meet the specific requirements of the particular application, water hardness, and environmental regulations [5–7].

In recent years, research has prominently focused on additives based on ionic liquids (ILs) and nanoparticles (NPs), highlighting their potential [8–10]. Emphasis has been placed on environmentally benign additives, particularly on exploring halogen-free ILs [11,12]. Numerous investigations have validated that ILs can establish adsorbed and chemisorbed layers on interacting surfaces, significantly reducing friction and wear [13]. A few papers reported that applying ILs resulted in superlubricity [14–16]. On the other hand, incorporating NPs into lubricants has emerged as a cutting-edge approach to enhance performance and efficiency [17,18]. Due to their unique physical and chemical properties, NPs offer a range of benefits, including friction and wear reduction, enhancement of load-carrying capacity, improved cooling capacity, restoring worn surfaces [19–22], etc. Among the

above-listed benefits of NPs, wear and friction reduction contribute to the longevity and efficiency of lubricated equipment. There was an in-depth analysis of tribological mechanisms, which include rolling, mending, protective film formation, surface polishing, third body, exfoliation, sharing, and tribo-sintering, etc. [18,23–26]. Even though the lubrication mechanism is closely related to the shape and nature of NPs, there are no general rules in the behaviour of particular NPs.

Combining ILs and NPs leverages their advantages, offering superior tribological performance [27–31]. Sanes et al. demonstrated that merging graphene nanoparticles with imidazolium IL in isoparaffinic base oil significantly improved surface separation and resulted in negligible wear [32]. These studies collectively affirm the benefits of synergy, often amplifying the effectiveness of the individual components.

Most research concerning hybrid additives has been directed towards oil-based lubricating fluids, with a scant number of investigations elucidating the synergistic effects of NPs and ILs in water-based lubricating systems. Carrion et al. elucidated that incorporating hybrid additives, consisting of diprotic ammonium palmitate IL together with nanodiamonds, enhanced the film thickness and lubricity in the water-based systems [33]. Similarly, Hao et al. corroborated that adding hybrid additives containing ILs and NPs improved the lubricity of water-based lubricating fluids [34]. The underlying synergistic mechanisms, attributed to micro-rolling, polishing, and mending activities, account for the observed improvement in lubricity. Some studies also suggest that the lubricity of NPs and ionic liquids modified water-based lubricating fluids can benefit from hydration layers [35].

This research examines the tribological characteristics of hybrid additives designed to improve the lubricating performance of the glycerol–water mixture. These hybrid additives comprise the protic ionic liquid and titanium oxide nanoparticles, with the ionic liquid being utilized either alone or synergistically with the nanoparticles.

2. Materials and Methods

2.1. Protic Ionic Liquid

Bis(2-hydroxyethyl)ammonium erucate (DEE) was synthesized following the procedure described in our previous study [36]. An acid-base neutralization reaction occurs between erucic acid and bis(2-hydroxyethyl)amine, forming a protic ionic liquid. The synthesis reaction was conducted at 90 °C for 24 h. Erucic acid (CAS No. 112-86-7) was sourced from Alfa Aesar, Germany, while Bis(2-hydroxyethyl)amine (CAS No. 111-42-2) was procured from Acros Organics, Germany. All analytical-grade reagents were used without further purification.

2.2. Preparation of Lubricating Samples

This study combined titanium (IV) dioxide nanoparticles with the protic ionic liquid. The NPs were sourced from Sigma-Aldrich and were used without additional preparation. Their specifications are presented in Table 1.

Table 1. Specifications of investigated titanium oxide NPs.

Investigated Nanoparticles, CAS No., and Abbreviation	Appearance	Particle Size, nm	Molecular Weight, g/mol	Trace Metals, %
Titanium (IV) oxide 13463-67-7 [TiO]	White powder	21	79.87	≥99.5

First, 15 mL samples containing 0.25 wt. % of NPs in water were dispersed using ultrasonication for 90 min in the Bandelin SONOREX TM RK 514 H ultrasonic cleaner operating in the following parameters: power—880 W, temperature—≤45 °C. Further, the samples were subjected to 10 min of centrifugation in the Thermo Scientific™ Multifuge X3R (Thermo Fisher) centrifuge to remove undispersed agglomerates. The centrifugation

parameters: rotation speed—4700 rpm, temperature—20 °C. The obtained supernatant was used to formulate lubricating samples. The principal preparation scheme is presented in Figure 1, while the detailed explanation of the preparation was described in our previous study [30].

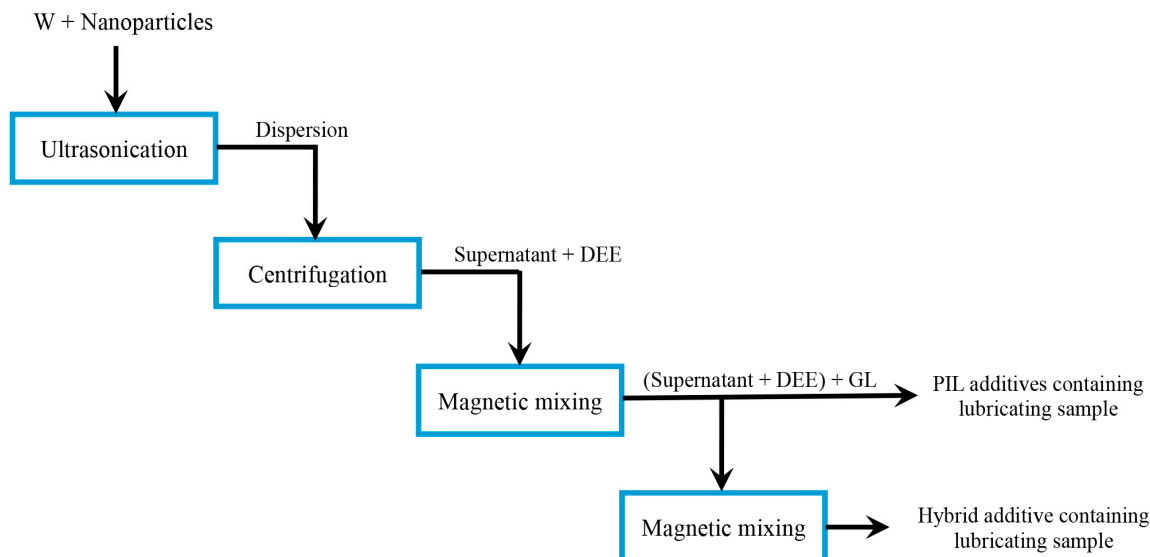


Figure 1. The principle scheme of the preparation of lubricating samples.

The synthesized DEE was incorporated as an additive in a glycerol–water mixture (WGL), where glycerol contained 50% by wt. The anhydrous glycerol was purchased from Acros Organics (Germany). The deionized water of resistance 3–5 MΩ was obtained using a filter system. Solutions with 0.125, 0.25, 0.5, 1, 2, and 3 wt. % of DEE in the base fluid were prepared by a magnetic mixer operating at 300 rpm at 40 °C. The mixing process yielded a light-yellow opaque solution, with an increase in opacity correlative to the concentration of DEE. Figure 2 depicts the visual characteristics of the resulting solutions. Inspection of the image clearly indicates that bis(2-hydroxyethyl)ammonium erucate exhibits solubility in water across the studied concentration spectrum. Furthermore, the solution demonstrated stability, exhibiting neither sedimentation nor clouding over an extended period of several days.

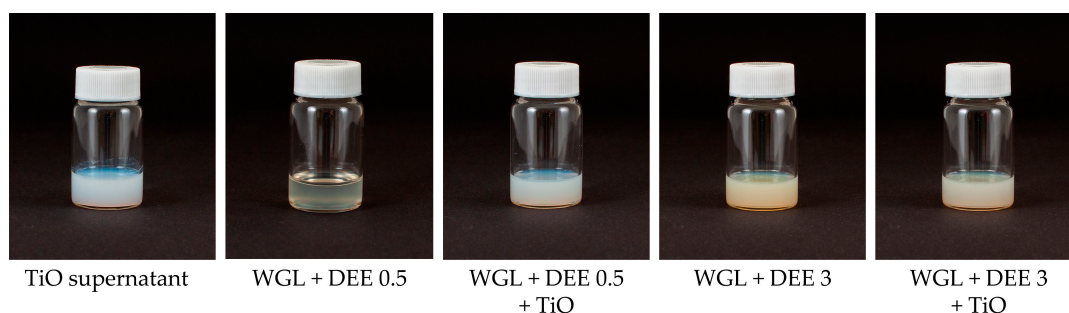


Figure 2. The visual characteristics of the formulated lubricant samples.

The lubricating samples containing hybrid additives were prepared by combining NPs and DEE. In this case, titanium oxide supernatant was loaded with an appropriate amount of DEE and stirred on a magnetic stirrer at 400 rpm for 30 min, maintaining 40 °C. After dissolving DEE, the glycerol was incorporated into the solution, and the mixture was stirred using the procedure described above. There was a single concentration of NPs, while protic ionic liquid had two concentrations, which were chosen based on the tribological results obtained when DEE was used alone. The samples contained 0.5% and 3% of DEE and the same amount of NPs. The visual characteristics of lubricating samples

containing hybrid additives are presented in Figure 2. The samples involving NPs have a white shade from titanium oxide. The titanium oxide supernatant was opaque white.

2.3. Physicochemical Properties and Rust Prevention Ability

The kinematic viscosity and density of investigated samples were examined at the same temperature at which tribo-tests were performed, namely, 30 °C. The SVM 3000 Anton Paar viscometer was used to test kinematic viscosity and density. The pH was measured using the Thermo Scientific Orion apparatus. For all the mentioned tests, three repetitions were made for each sample.

The rust prevention efficacy of cast iron was assessed following the ASTM D4627 standard test method. In this assay, 5 g of cast iron chips were evenly spread on a white filter paper and positioned in a 100 mm diameter petri dish. Each petri dish received 5 mL of the tested sample to ensure that the filter paper was fully submerged. The petri dishes, covered, were then stored at ambient temperature for 24 h, shielded from direct sunlight. Subsequently, the chips were meticulously removed, and the filter paper was cleansed with running water. Photographs documenting the corrosion spots were captured and analyzed. Samples demonstrating better rust prevention displayed fewer corrosion marks on the filter paper. Each sample underwent at least two independent trials.

2.4. Tribo-Tests and Worn Surface Analysis

The tribological characteristics of the samples were evaluated utilizing a ball-on-plate reciprocating tribometer, model TR-282, from Ducom, India. The tribo-test conditions are briefly summarized in Table 2. A 6 mm diameter ball was rubbed against a plate during the tribo-test. The plate was made of bearing steel 100Cr6 having a hardness of 190 HV and roughness Ra—0.02 µm. Two different ball materials were used: (i) ceramic ball Al₂O₃ (Alumina), hardness—1550 HV, roughness Ra—0.025 µm; and (ii) tungsten carbide (WC), hardness—1300 HV, roughness—Ra—0.03 µm. The quality of both balls was from the 25th grade. Variations in the coefficient of friction (COF) were recorded during the tribological testing. The mean value of the COF was determined from data collected during the final 20 min of the test.

Table 2. Summary of tribo-test parameters.

Test Temperature, °C	Test Duration, min	Stroke Length, mm	Load, N	Amount of Lubricating Sample, mL	Reciprocation Frequency, Hz
30	30	1	4	1	15

The worn surfaces were examined using a Nikon ECLIPSE MA 100 (Japan) optical microscope and a Hitachi 3400N scanning electron microscope (SEM). Bruker Quad 5040 energy-dispersive spectroscopy (EDS) was employed to analyze the composition of worn surfaces. Before inspection, the specimens were cleaned using toluene and acetone. The cross-sectional profiles of the wear traces were quantified at various points along the traces with a Mahr GD-25 stylus profilometer. These measurements calculated the areas of the cross-sectional profiles and the wear volumes.

The evaluation of lubricity primarily focused on three criteria: the coefficient of friction, wear volume, and the morphological characteristics of the worn surfaces.

3. Results and Discussion

3.1. Physicochemical Properties and Rust Prevention Ability of Prepared Lubricating Samples

Kinematic viscosity and pH are essential parameters that influence the performance of the lubricating fluid. Higher viscosity leads to better lubricity, while lower-viscosity fluids achieve better cooling capacity. As a rule of thumb, the viscosity of WBLFs is kept between 2 and 20 mm²/s at 40 °C. All the investigated samples are found at this interval in the

present study. The presence of protic ionic liquid governed the viscosity of the analyzed samples. The kinematic viscosity increases with increased DEE (Table 3).

Table 3. Physicochemical characteristics of investigated lubricating samples.

Lubricating Sample	Kinematic Viscosity @ 30 °C, mm ² /s	Density @ 30 °C, g/cm ³	pH
WGL	3.842 ± 0.004	1.121 ± 0.0001	8.03 ± 0.013
WGL+DEE 0.125	4.061 ± 0.003	1.123 ± 0.0003	8.46 ± 0.007
WGL+DEE 0.25	4.336 ± 0.020	1.122 ± 0.0002	8.52 ± 0.005
WGL+DEE 0.5	4.880 ± 0.042	1.121 ± 0.0002	8.63 ± 0.011
WGL+DEE 1	5.330 ± 0.033	1.119 ± 0.0003	8.88 ± 0.012
WGL+DEE 2	6.440 ± 0.049	1.118 ± 0.0001	9.16 ± 0.007
WGL+DEE 3	8.094 ± 0.067	1.117 ± 0.0002	9.20 ± 0.007
WGL+DEE 0.5 + TiO ₂	4.916 ± 0.015	1.122 ± 0.0002	8.60 ± 0.013
WGL+DEE 3 + TiO ₂	8.272 ± 0.021	1.116 ± 0.0003	9.13 ± 0.009

On the other hand, the introduction of nanoparticles only marginally increased the viscosity. The pH of the lubricating fluid must be kept within an optimal range to prevent corrosion and microbial growth. Generally, the optimal pH range for WBLFs is between 8.5 and 9.5 [4]. The introduction of DEE increased pH, while NPs slightly reduced it.

The corrosion prevention ability is one of the main properties desirable in any application where steel surfaces are subjected to contact with WBLFs [37]. Lubricants should offer protection against corrosion, usually carried out by forming a barrier between the metal surface and corrosive elements. The present study used cast iron chips to inspect the corrosion prevention ability. The corroded cast iron chips transferred corrosion marks on filter paper. The images of the filter papers are presented in Figure 3.

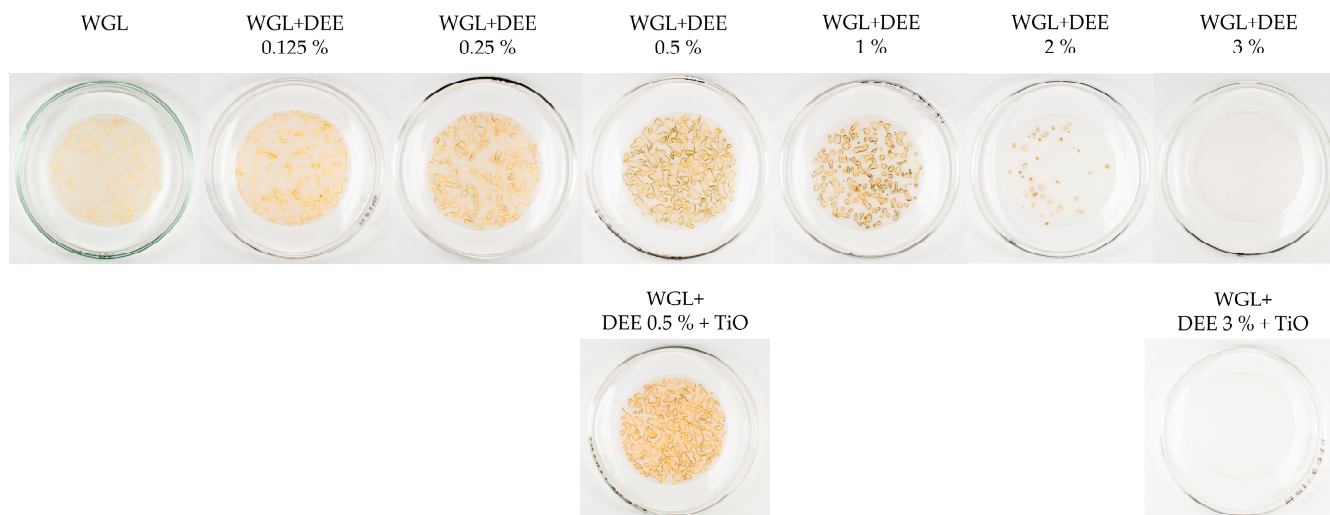


Figure 3. The appearance of corrosion marks on filter paper after the corrosion test when the aqueous glycerol solution was modified with different concentrations of DEE and NPs.

It was evident that glycerol aqueous solution cannot prevent corrosion of cast iron chips. Therefore, chips immersed in this medium show mild corrosion. The introduction of investigated protic ionic liquid encouraged corrosion. The most intense corrosion was observed using a solution containing 0.5% DEE. Fortunately, a further increase in DEE concentration eliminated the corrosion. It was found that 3% of DEE-containing lubricating fluid prevents corrosion. The introduction of NPs did not affect corrosion prevention behaviour. The hybrid additive containing samples with 0.5% DEE still showed many corrosion marks, while samples with 3% DEE showed no corrosion. According to findings

reported in the literature, nitrogen-containing compounds can adsorb on metal surfaces, forming a protective layer [4,38]. This layer reduces the access to oxygen, thus reducing corrosion. Therefore, it can be stated that investigated hybrid additives can be used as corrosion prevention additives for WBLFs and coolants.

3.2. Lubricity of Protic Ionic Liquid Additive

According to our previous studies and reports from other scholars, protic ionic liquids provide superior lubricity to aqueous lubricants [6,12,39]. Therefore, this study investigated the performance of ionic liquid alone before its combination with NPs. The mean coefficient of friction and wear volume observed when glycerol aqueous solution was loaded with protic ionic liquid are presented in Figure 4. The lubrication with additive-free base fluid produced high COF for both friction pairs. The COF was significantly reduced with the introduction of DEE (Figure 4a). In the case of a tungsten carbide ball, the COF was decreased to 0.08 and showed no significant variation with an increased concentration of DEE. On the other hand, the lubrication of the alumina ball containing friction pair underwent more improvement when a higher concentration of DEE was applied. Lubrication of the Alumina/Bearing steel friction pair showed the lowest COF of 0.06 using the lubricating sample containing 0.5% DEE.

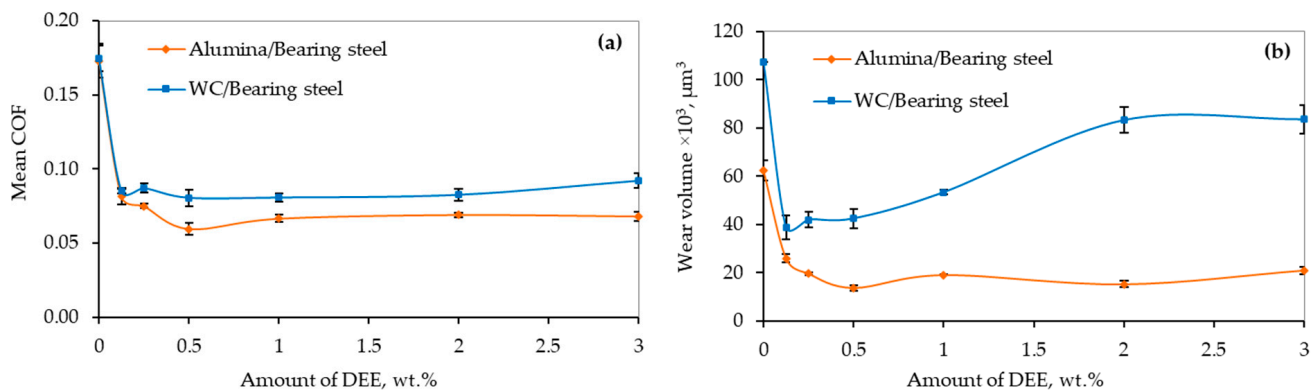


Figure 4. The variation in the mean COF (a) and wear volume (b) as a function of the amount of protic ionic liquid in base fluid observed while lubricating different friction pairs.

A more pronounced difference between the lubrication of investigated friction pairs arises when comparing wear results (Figure 4b). The lubrication of the tungsten carbide ball containing friction pair was improved significantly by introducing the most minor DEE concentration. In particular, introducing 0.125% of DEE resulted in a 2.76 times wear reduction. The increase in the amount of DEE up to 0.5% has no significant influence. However, a further increase of up to 3% leads to increased wear. The increased wear while the friction is low points out the process of tribo-corrosion. In that case, the wear is governed by the continuous removal of the upper softened layer. This process is not energy-hungry. Therefore, COF remains low [40].

The Alumina/Bearing steel friction pair underwent less wear than the WC/Bearing steel. It showed less wear when additive-free base fluid was used, and the wear was further reduced with the introduction of DEE. The lowest wear in the Alumina/Bearing steel friction pair was observed when modifying base fluid with 0.5% DEE. It was 4.5 times lower than the additive-free sample and three times lower than the lowest value observed in the WC/Bearing steel friction pair. Evidently, the material of the counter body plays a significant role in friction and wear, whereas inert ceramic has an advantage. It is reported that ceramic materials can form smoother surfaces when interacting with steel, reducing adhesion and adhesive wear. Moreover, ceramics' hardness and lower tendency to adhere to steel reduce adhesive and abrasive wear [41].

Figure 5 presents the COF variation during the tribo-tests. The DEE-loaded samples exhibited stable COF throughout the test. Despite the concentration, DEE-loaded samples have similar variation patterns. There was also a marginal difference between investigated friction pairs. The significant difference occurred only when additive-free base fluid was examined and compared. Although the COF was slightly higher in the WC/Bearing steel friction pair, it was more stable when additive-free base fluid was used.

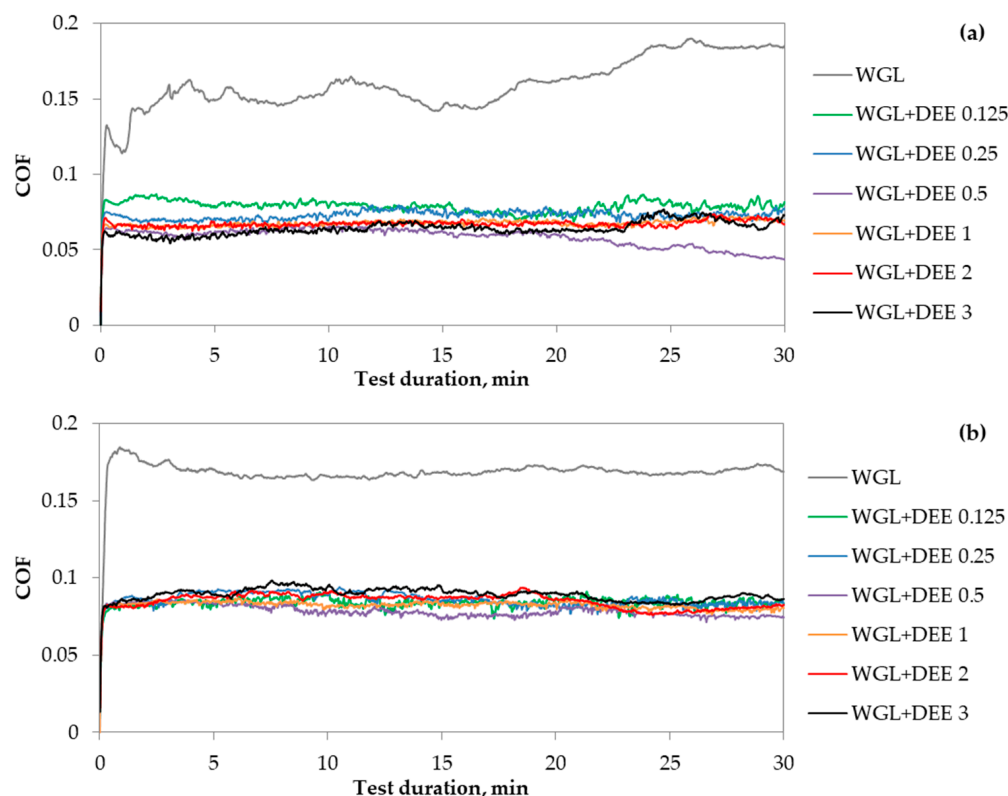


Figure 5. Fluctuations in the coefficient of friction over the course of testing time when (a) Alumina/Bearing steel and (b) WC/Bearing steel friction pairs were lubricated with additive-free and DEE-loaded base fluid.

A distinct feature of the 0.5% DEE-loaded sample was observed when it was used to lubricate the Alumina/Bearing steel friction pair. After 20 min of performing the tribo-test, the COF started to decrease, obtaining a COF value as low as 0.045 at the end of the test. This particular concentration could be the subject of further studies as it also possesses the lowest wear.

The appearance of the worn surfaces supplements the results mentioned above. The lubrication of both friction pairs resulted in slight polishing of the ball surface (Figures 6 and 7). Only in the case of additive-free base fluid were abrasion marks discerned on the balls. When low wear was observed, the wear scars on the balls were difficult to determine. This is mainly the case for lubricating the Alumina/Bearing steel friction pair with a sample having 0.5% DEE (Figure 5).

The wear traces on the plate exhibited minimal polishing when DEE was introduced at any studied concentration. Slightly more abrasion occurred when the WC ball slid against the bearing steel plate. Figures 6 and 7 also provide corresponding cross-sectional profiles of the wear traces. The lubrication with WGL resulted in high abrasion on the plate surface when the Alumina ball was used. In contrast, the worn surface observed after lubricating the WC/Bearing steel friction pair is relatively smooth. The difference in worn surface appearance correlates with COF variation, where the WC ball having friction pair shows more stable COF (Figure 5).

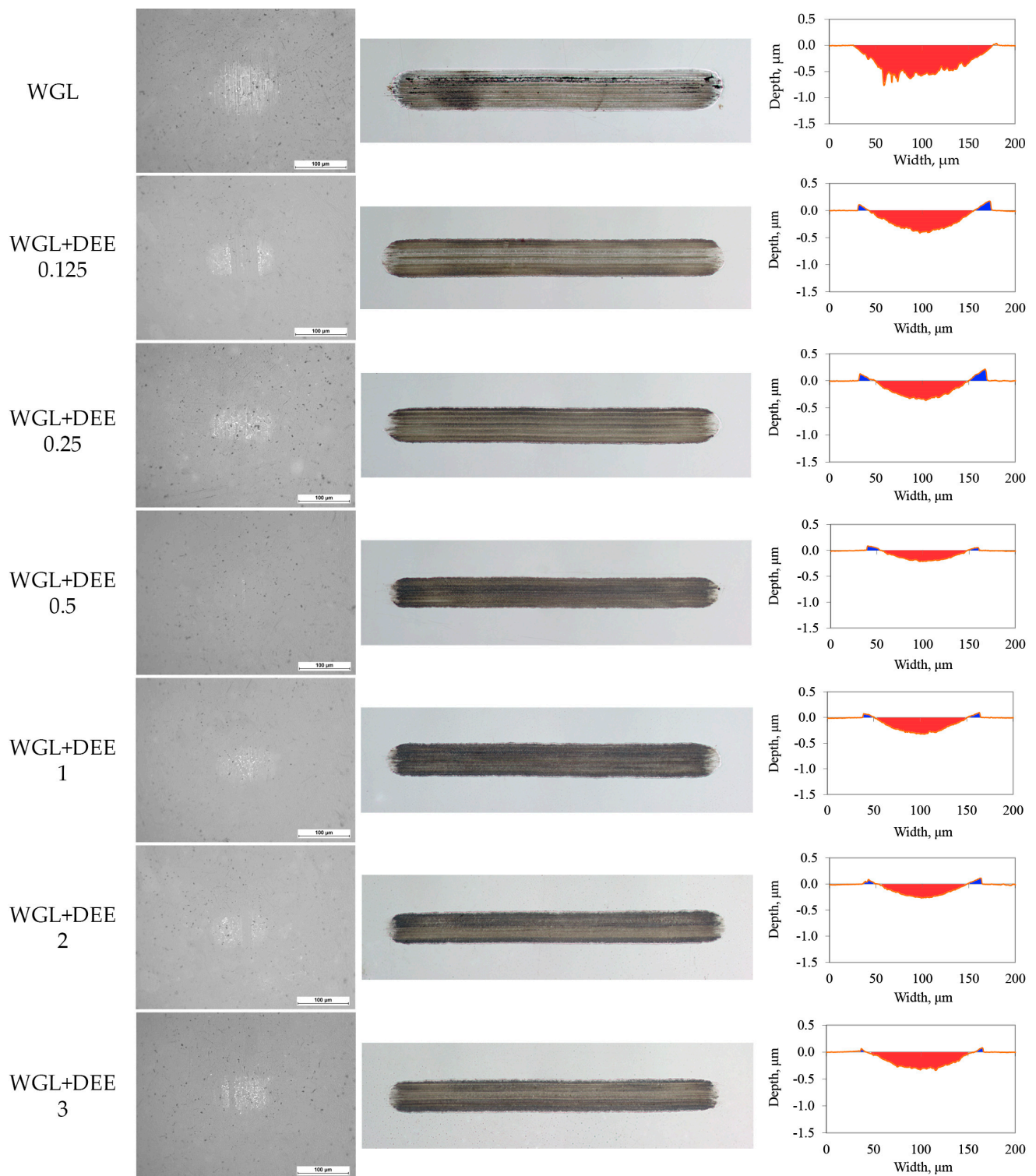


Figure 6. The effect of DEE concentration on the appearance of wear marks after tribo-test of the Alumina/Bearing steel friction pair. From left to right, the sequence includes the wear scar on the ball, the wear trace on the plate, and the cross-sectional profile of the trace.

The application of DEE resulted in the appearance of pushed-out material at the edges of the wear traces. Except for lubrication with additive-free base fluid, the pushed-out material increases with increased wear. This behaviour characterizes both friction pairs.

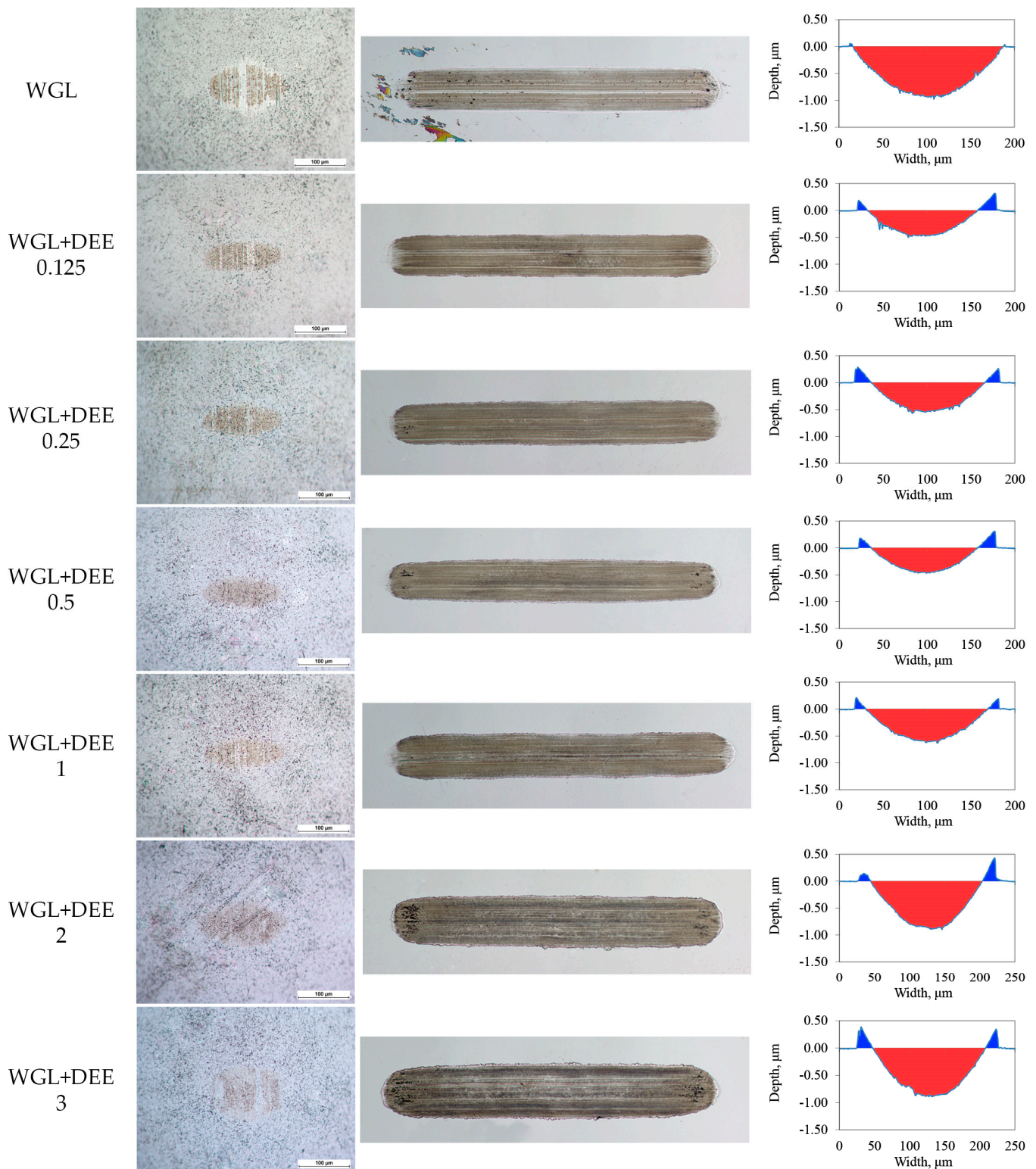


Figure 7. The effect of DEE concentration on the appearance of wear marks after tribo-test of the WC/Bearing steel friction pair. From left to right, the sequence includes the wear scar on the ball, the wear trace on the plate, and the cross-sectional profile of the trace.

Lubricating the WC/Bearing steel friction pair with DEE-loaded samples resulted in adhesion marks at the ends of the wear traces. This was particularly evident when higher concentrations of DEE were used. Namely, these wear traces also suffered more abrasion.

3.3. Lubricity of Hybrid Additives

The application of hybrid additives provided base fluid with different lubricity features. This section will compare the lubricity of hybrid additive-loaded WGL with that described above, where 0.5 and 3% of DEE additive-containing WGL was investigated. The comparison of COF variation when DEE was used alone and together with NPs is presented in Figure 8. Although the mean COF increased when hybrid additives were used to lubricate the Alumina/Bearing steel friction pair, the COF became more stable. The stabilizing effect can also be discerned in the case of the WC/Bearing steel friction pair lubrication. However, this friction pair's difference between mean COF values is negligible. Therefore, it can be stated that the application of hybrid additives stabilizes the friction process in both friction pairs.

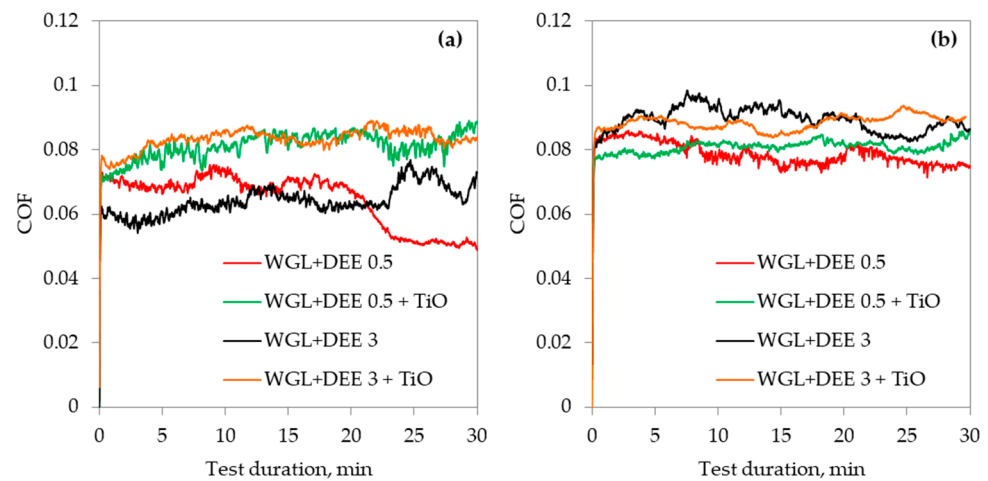


Figure 8. Fluctuations in the coefficient of friction over the course of testing time when (a) Alumina/Bearing steel and (b) WC/Bearing steel friction pairs were lubricated with DEE and hybrid additives.

Associated with the higher coefficient of friction (COF), using hybrid additives led to a decreased wear reduction in the Alumina/Bearing steel friction pair, as shown in Figure 9a. The wear volume increased for both DEE concentrations when combined with nanoparticles (NPs), showing that wear was not influenced by the concentration of DEE. Introducing a hybrid additive reduced wear by 1.85 times compared to the wear observed with the additive-free base fluid.

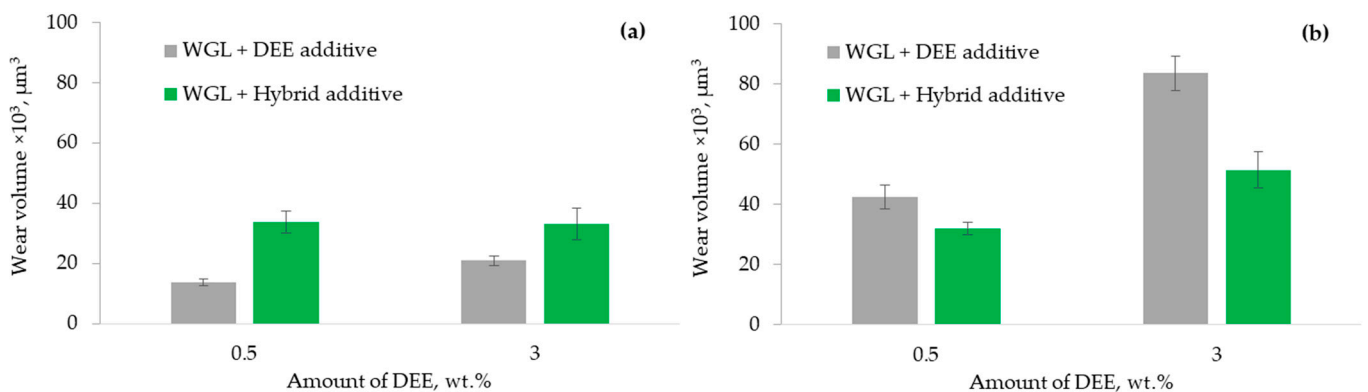


Figure 9. The wear volume of (a) Alumina/Bearing steel and (b) WC/Bearing steel friction pairs after lubrication with DEE and hybrid additives.

On the other hand, hybrid additives used to lubricate the WC/Bearing steel friction pair improved wear reduction. Compared to additive-free base fluid, the positive effect was observed for both DEE concentrations, resulting in 3.4 and 2.1 times improvement

for 0.5 and 3% of DEE, respectively. Correspondingly, it is a 28.7 and 47.9% improvement compared to the results observed when the DEE additive was used alone.

Figures 10 and 11 present the worn surfaces produced when hybrid additives were used to enhance lubricity. The ball surface underwent slight polishing in both friction pairs, and a tribo-film formation was seen in all the investigated cases. In the case of the Alumina/Bearing steel friction pair, the wear trace on the plate evidences higher wear, but the worn surface is smothered (Figure 10). There is also a larger volume of pushed-out material than when only the DEE additive was used.

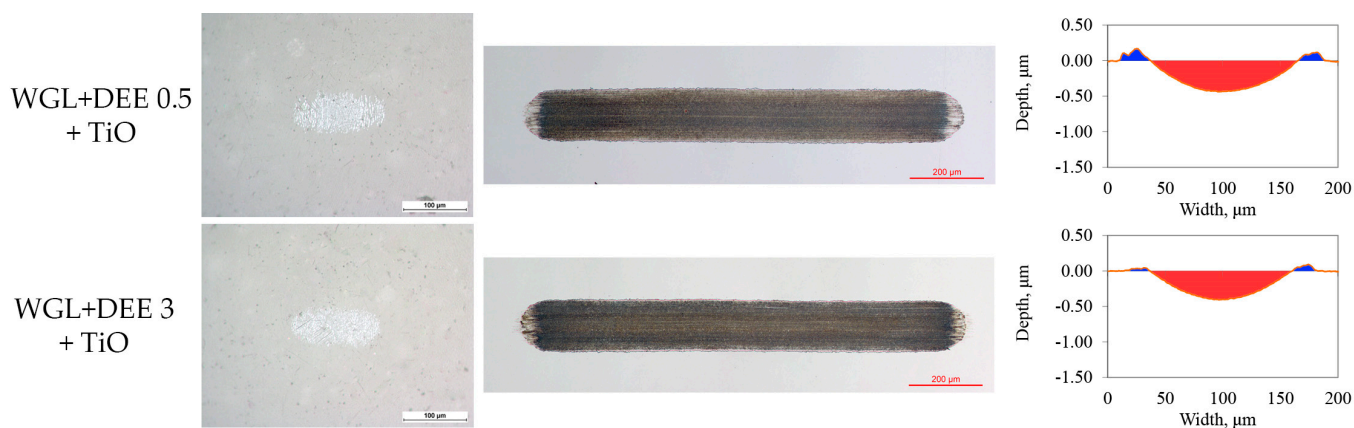


Figure 10. The effect of hybrid additives on the appearance of wear marks after tribo-test of the Alumina/Bearing steel friction pair. From left to right, the sequence includes the wear scar on the ball, the wear trace on the plate, and the cross-sectional profile of the trace.

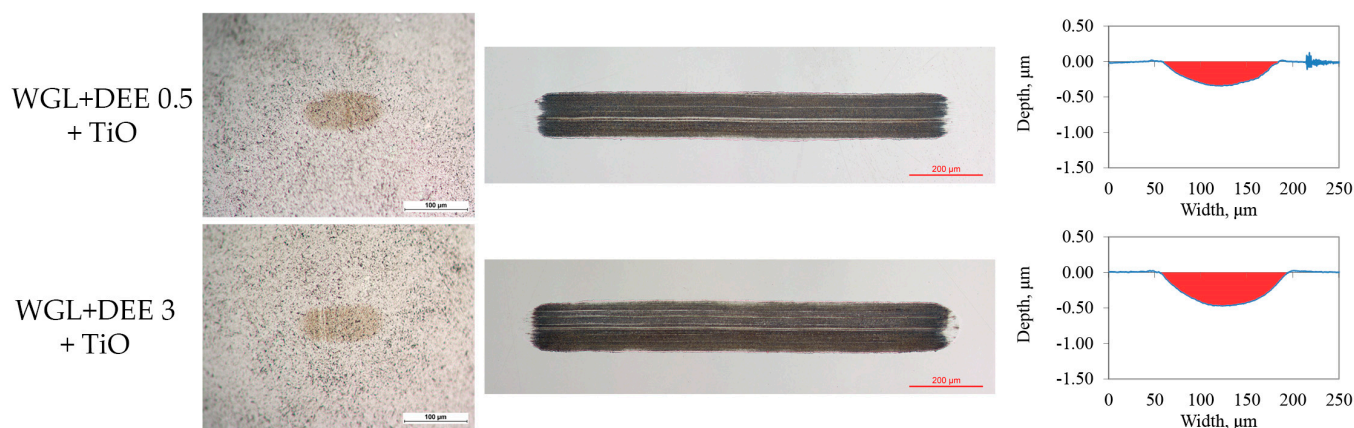


Figure 11. The effect of hybrid additives on the appearance of wear marks after tribo-test of the WC/Bearing steel friction pair. From left to right, the sequence includes the wear scar on the ball, the wear trace on the plate, and the cross-sectional profile of the trace.

Applying hybrid additives resulted in more changes in the WC/Bearing steel friction pair. The worn surfaces appear less damaged than those observed when only the DEE additive was used (Figures 7 and 11). Moreover, the pushed-out material at the sides of the wear trace is negligible. These changes are reflected in the wear reduction results, where less wear was observed. For both friction pairs, the smooth surfaces correlate with COF variation.

For the WC/Bearing steel friction pair, the most pronounced characteristics appeared at the ends of the wear traces, specifically where the reciprocating ball alters its sliding direction. These areas experienced particularly severe lubrication conditions. Utilizing a base fluid without additives led to adhesion between the interacting surfaces, as depicted in Figure 12a. The adhesion was also evident in the whole wear trace, as seen in Figure 7. The

adhered particles caused three-body abrasion on the relatively soft plate surface. Introducing protic ionic liquid reduced the adhesion and abrasion (Figure 12b,d). However, minor adhesion marks can still be found at the ends of the wear trace. The appearance of wear trace changed significantly when protic ionic liquid was used together with nanoparticles (Figure 12c,e). By using hybrid additives, the adhesion was eliminated, and abrasion was reduced. It could be that NPs acted as rolling elements, thus preventing direct contact between interacting surfaces and stabilizing friction [42,43]. However, Figure 12c,e show that tribo-film was removed from the very end of the wear trace. Maybe at a low speed, titanium oxide NPs have a polishing effect. Some papers reported the sintering as an action mechanism of titanium oxide NPs [42].

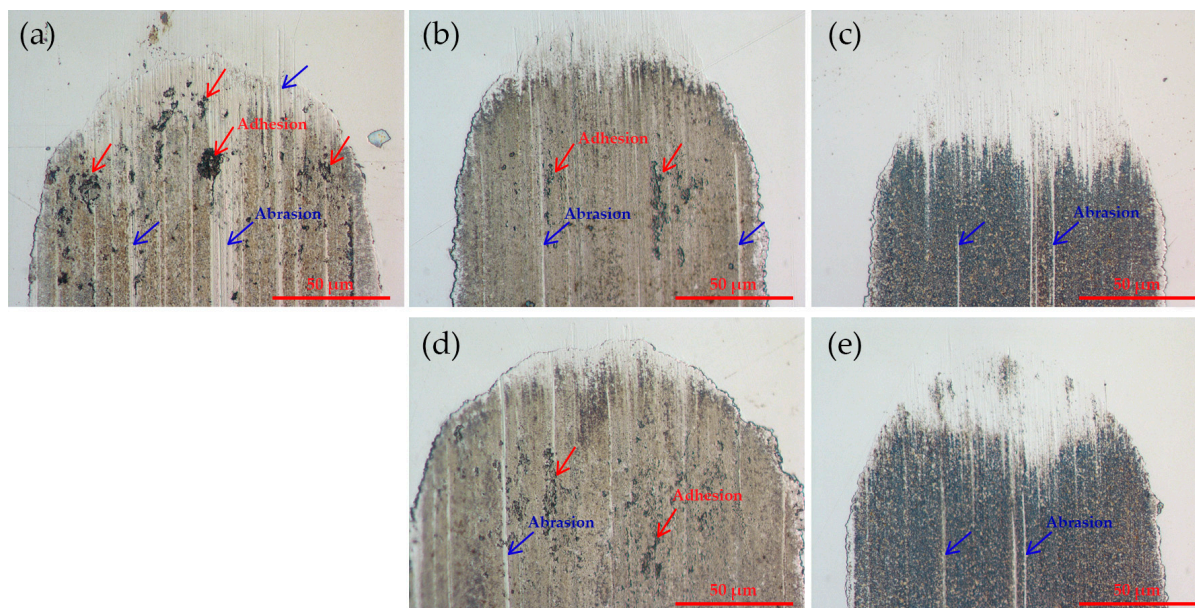


Figure 12. The end region of the wear trace observed in the WC/Bearing steel friction pair after tribo-test when lubricating with (a) WGL, (b) WGL+DEE 0.5, (c) WGL+DEE 0.5 + TiO, (d) WGL+DEE 3, and (e) WGL+DEE 3 + TiO.

The SEM and EDS analyses were performed to analyze the lubricity mechanisms further. The high-magnification images of worn surfaces and the edges of the wear trace on the plate are presented in Figures S1 and S2. The appearance of worn surfaces is similar in all additive-loaded samples. The prevailing feature is a grainy structure. The difference is the pushed-out material, which is smaller when low wear is observed. The EDS analysis shows that all worn surfaces comprise an increased amount of oxygen, carbon, and nitrogen. In addition, hybrid additives lubricated surfaces contain titanium (Figures S1 and S2). There was no characteristic element distribution for a particular friction pair or DEE concentration (Tables S1 and S2). After lubrication with additive-loaded samples, the worn surfaces contained oxygen—2.9 . . 5.5%; carbon—0.5 . . 2.21%; and nitrogen—1.2 . . 4.8%. In the case of hybrid additives, worn surfaces also had 0.85 . . 1.25% titanium.

Evidently, the worn surfaces were oxidized and contained residue tribo-film comprising carbon and nitrogen. It is evident from other studies that protic ionic liquid tends to form an adsorption layer on the interacting surfaces [44]. Adsorbed layers react with the metal surface, creating friction polymers or metal soaps [45,46]. In this way, the surfaces separating tribo-film are generated, preventing direct interaction. The introduction of titanium oxide NPs resulted in changed lubricity conditions. In the case of the Alumina/Bearing steel friction pair, the wear reduction was diminished if compared to that obtained without nanoparticles. On the other hand, introducing a hybrid additive resulted in the further wear reduction of the WC/Bearing steel friction pair. According to the views of optical images and surface composition, the rolling and tribo-sintering of nanoparticles could

be involved in tribo-film formation. A similar phenomenon was suggested in the other reports [17,42,47].

4. Conclusions

This study formulated the hybrid lubricity-improving additives by combining protic ionic liquid and nanoparticles. The tribological properties of formulated lubricating samples were investigated on two friction pairs—Alumina/Bearing steel and WC/Bearing steel on reciprocating ball-on-plate tribometer. Considering the results presented above, the following conclusions can be drawn:

1. Bis (2-hydroxyethyl)ammonium erucate protic ionic liquid prevented corrosion when used as an additive in glycerol aqueous solutions. Corrosion was eliminated by loading base fluid with 3 wt. % of protic ionic liquid. The introduction of nanoparticles did not change this behaviour.
2. Bis(2-hydroxyethyl)ammonium erucate protic ionic liquid improved the lubricity of water-based lubricating fluid by a few orders of magnitude. A greater improvement was achieved in lubricating the Alumina/Bearing steel friction pair. It was found that 0.5 wt. % concentration of the investigated ionic liquid in the base fluid was the most effective.
3. The application of the hybrid additive improved lubricity when it was used to lubricate the WC/Bearing steel friction pair. On the other hand, the lubricity of the Alumina/Bearing steel friction pair diminished.
4. It was proposed that the adsorption layer of protic ionic liquid molecules was responsible for preventing corrosion and improving lubricity. During the tribo-interaction, the adsorbed layer could react with metal surfaces, forming either friction polymer or metal soap. With the introduction of titanium oxide, the lubrication mechanism could involve rolling and tribo-sintering of nanoparticles.
5. Even though further studies are necessary to understand the lubricity of suggested hybrid additives in various friction pairs, the presented results could be interesting for those who seek environmentally friendly alternatives.

Supplementary Materials: The following supporting information can be downloaded at: <https://www.mdpi.com/article/10.3390/lubricants12050178/s1>, Figure S1. SEM images of the wear traces in the Alumina/Bearing steel friction pair and EDS graphs obtained when measuring the composition in the wear traces. Figure S2. SEM images of the wear traces in the WC/Bearing steel friction pair and EDS graphs obtained when measuring the composition in the wear traces. Table S1. Atomic [%] composition of the wear traces on the plate observed after lubrication of Alumina/Bearing steel friction pair with protic ionic liquid and hybrid additive modified base fluid. Table S2. Atomic [%] composition of the wear traces on the plate observed after lubrication of WC/Bearing steel friction pair with protic ionic liquid and hybrid additive modified base fluid.

Author Contributions: Conceptualization, R.K.; methodology, R.K. and A.K.; validation, R.K., M.G. and A.K.; formal analysis, R.K. and E.S.; investigation, M.G., A.K. and J.T.; resources, E.S.; writing—original draft preparation, R.K. and E.S.; writing—review and editing, R.K. and E.S.; visualization, J.T., R.K. and M.G.; supervision, E.S. and R.K.; project administration, R.K.; funding acquisition, E.S. All authors have read and agreed to the published version of the manuscript.

Funding: This research was funded by grant No. S-MIP-21-61 from the Research Council of Lithuania.

Data Availability Statement: Data are contained within the article.

Conflicts of Interest: The authors declare no conflicts of interest.

References

1. The Business Research Company. *Metalworking Fluids Global Market Report 2024*; The Business Research Company: Hyderabad, India, 2023.
2. Nune, M.M.R.; Chaganti, P.K. Development, Characterization, and Evaluation of Novel Eco-Friendly Metal Working Fluid. *Measurement* **2019**, *137*, 401–416. [[CrossRef](#)]

3. Gajrani, K.K.; Suvin, P.S.; Kailas, S.V.; Mamilla, R.S. Thermal, Rheological, Wettability and Hard Machining Performance of MoS₂ and CaF₂ Based Minimum Quantity Hybrid Nano-Green Cutting Fluids. *J. Mater. Process. Technol.* **2019**, *266*, 125–139. [[CrossRef](#)]
4. Gajrani, K.K.; Suvin, P.S.; Kailas, S.V.; Sankar, M.R. Hard Machining Performance of Indigenously Developed Green Cutting Fluid Using Flood Cooling and Minimum Quantity Cutting Fluid. *J. Clean Prod.* **2019**, *206*, 108–123. [[CrossRef](#)]
5. Najiha, M.S.; Rahman, M.M.; Yusoff, A.R. Environmental Impacts and Hazards Associated with Metal Working Fluids and Recent Advances in the Sustainable Systems: A Review. *Renew. Sustain. Energy Rev.* **2016**, *60*, 1008–1031. [[CrossRef](#)]
6. Yang, Z.; Sun, C.; Zhang, C.; Zhao, S.; Cai, M.; Liu, Z.; Yu, Q. Amino Acid Ionic Liquids as Anticorrosive and Lubricating Additives for Water and Their Environmental Impact. *Tribol. Int.* **2021**, *153*, 106663. [[CrossRef](#)]
7. Xie, G.; Liu, S.; Guo, D.; Wang, Q.; Luo, J. Investigation of the Running-in Process and Friction Coefficient under the Lubrication of Ionic Liquid/Water Mixture. *Appl. Surf. Sci.* **2009**, *255*, 6408–6414. [[CrossRef](#)]
8. Amiril, S.A.S.; Rahim, E.A.; Syahrullail, S. A Review on Ionic Liquids as Sustainable Lubricants in Manufacturing and Engineering: Recent Research, Performance, and Applications. *J. Clean Prod.* **2017**, *168*, 1571–1589. [[CrossRef](#)]
9. Nasser, K.I.; Liñeira del Río, J.M.; Mariño, F.; López, E.R.; Fernández, J. Double Hybrid Lubricant Additives Consisting of a Phosphonium Ionic Liquid and Graphene Nanoplatelets/Hexagonal Boron Nitride Nanoparticles. *Tribol. Int.* **2021**, *163*, 107189. [[CrossRef](#)]
10. Nasser, K.I.; Liñeira del Río, J.M.; López, E.R.; Fernández, J. Hybrid Combinations of Graphene Nanoplatelets and Phosphonium Ionic Liquids as Lubricant Additives for a Polyalphaolefin. *J. Mol. Liq.* **2021**, *336*, 116266. [[CrossRef](#)]
11. Avilés, M.D.; Pamies, R.; Sanes, J.; Arias-Pardilla, J.; Carrión, F.J.; Bermúdez, M.D. Protic Ammonium Bio-Based Ionic Liquid Crystal Lubricants. *Tribol. Int.* **2021**, *158*, 106917. [[CrossRef](#)]
12. Kreivaitis, R.; Gumbyté, M.; Treinytė, J. Investigation of Tribological Properties of Environmentally Friendly Ionic Liquids as a Potential Lubricity Improving Additives for Water-Based Lubricants. *Ind. Lubr. Tribol.* **2022**, *74*, 294–301. [[CrossRef](#)]
13. Donato, M.T.; Colaço, R.; Branco, L.C.; Saramago, B. A Review on Alternative Lubricants: Ionic Liquids as Additives and Deep Eutectic Solvents. *J. Mol. Liq.* **2021**, *333*, 116004. [[CrossRef](#)]
14. Shekhar, H.; Dumpala, R. Overcoming Friction and Steps towards Superlubricity: A Review of Underlying Mechanisms. *Appl. Surf. Sci. Adv.* **2021**, *6*, 100175. [[CrossRef](#)]
15. Han, T.; Zhang, S.; Zhang, C. Unlocking the Secrets behind Liquid Superlubricity: A State-of-the-Art Review on Phenomena and Mechanisms. *Friction* **2022**, *10*, 1137–1165. [[CrossRef](#)]
16. Han, T.; Yi, S.; Zhang, C.; Li, J.; Chen, X.; Luo, J.; Banquy, X. Superlubrication Obtained with Mixtures of Hydrated Ions and Polyethylene Glycol Solutions in the Mixed and Hydrodynamic Lubrication Regimes. *J. Colloid Interface Sci.* **2020**, *579*, 479–488. [[CrossRef](#)]
17. Azman, N.F.; Samion, S. Dispersion Stability and Lubrication Mechanism of Nanolubricants: A Review. *Int. J. Precis. Eng. Manuf.-Green Technol.* **2019**, *6*, 393–414. [[CrossRef](#)]
18. Nyholm, N.; Espallargas, N. Functionalized Carbon Nanostructures as Lubricant Additives—A Review. *Carbon N. Y.* **2023**, *201*, 1200–1228. [[CrossRef](#)]
19. Lee, G.J.; Rhee, C.K. Enhanced Thermal Conductivity of Nanofluids Containing Graphene Nanoplatelets Prepared by Ultrasound Irradiation. *J. Mater. Sci.* **2014**, *49*, 1506–1511. [[CrossRef](#)]
20. Sanukrishna, S.S.; Vishnu, S.; Jose Prakash, M. Experimental Investigation on Thermal and Rheological Behaviour of PAG Lubricant Modified with SiO₂ Nanoparticles. *J. Mol. Liq.* **2018**, *261*, 411–422. [[CrossRef](#)]
21. Gulzar, M.; Masjuki, H.; Varman, M.; Kalam, M.; Mufti, R.A.; Zulkifli, N.; Yunus, R.; Zahid, R. Improving the AW/EP Ability of Chemically Modified Palm Oil by Adding CuO and MoS₂ Nanoparticles. *Tribol. Int.* **2015**, *88*, 271–279. [[CrossRef](#)]
22. Dassenoy, F. Nanoparticles as Additives for the Development of High Performance and Environmentally Friendly Engine Lubricants. *Tribol. Online* **2019**, *14*, 237–253. [[CrossRef](#)]
23. Saini, V.; Bijwe, J.; Seth, S.; Ramakumar, S.S.V. Unexplored Solid Lubricity of Titanium Nanoparticles in Oil to Modify the Metallic Interfaces. *Appl. Surf. Sci.* **2022**, *580*, 152127. [[CrossRef](#)]
24. Kumar, R.; Gautam, R.K. Tribological Investigation of Sunflower and Soybean Oil with Metal Oxide Nanoadditives. *Biomass Convers. Biorefin.* **2024**, *14*, 2389–2401. [[CrossRef](#)]
25. Alves, S.M.; Mello, V.S.; Faria, E.A.; Camargo, A.P.P. Nanolubricants Developed from Tiny CuO Nanoparticles. *Tribol. Int.* **2016**, *100*, 263–271. [[CrossRef](#)]
26. Alves, S.M.; Barros, B.S.; Trajano, M.F.; Ribeiro, K.S.B.; Moura, E. Tribological Behavior of Vegetable Oil-Based Lubricants with Nanoparticles of Oxides in Boundary Lubrication Conditions. *Tribol. Int.* **2013**, *65*, 28–36. [[CrossRef](#)]
27. He, Z.; Alexandridis, P. Ionic Liquid and Nanoparticle Hybrid Systems: Emerging Applications. *Adv. Colloid Interface Sci.* **2017**, *244*, 54–70. [[CrossRef](#)] [[PubMed](#)]
28. Liñeira del Río, J.M.; López, E.R.; Fernández, J. Synergy between Boron Nitride or Graphene Nanoplatelets and Tri(Butyl)Ethylphosphonium Diethylphosphate Ionic Liquid as Lubricant Additives of Triisotridecyltrimellitate Oil. *J. Mol. Liq.* **2020**, *301*, 112442. [[CrossRef](#)]
29. Li, Y.; Zhang, S.; Ding, Q.; Li, H.; Qin, B.; Hu, L. Understanding the Synergistic Lubrication Effect of 2-Mercaptobenzothiazolate Based Ionic Liquids and Mo Nanoparticles as Hybrid Additives. *Tribol. Int.* **2018**, *125*, 39–45. [[CrossRef](#)]
30. Kreivaitis, R.; Treinytė, J.; Kupčinskis, A.; Gumbyté, M.; Andriušis, A. Improving Tribological Properties of Water/Glycerol Lubricating Fluid by the Synergy of Nanoparticles and Protic Ionic Liquid. *Wear* **2023**, *534*, 205133. [[CrossRef](#)]

31. Upendra, M.; Vasu, V. Synergistic Effect Between Phosphonium-Based Ionic Liquid and Three Oxide Nanoparticles as Hybrid Lubricant Additives. *J. Tribol.* **2020**, *142*, 052101. [[CrossRef](#)]
32. Sanes, J.; Avilés, M.D.; Saurín, N.; Espinosa, T.; Carrión, F.J.; Bermúdez, M.D. Synergy between Graphene and Ionic Liquid Lubricant Additives. *Tribol. Int.* **2017**, *116*, 371–382. [[CrossRef](#)]
33. Carrión, F.J.; Avilés, M.D.; Nakano, K.; Tadokoro, C.; Nagamine, T.; Bermúdez, M.D. Diprotic Ammonium Palmitate Ionic Liquid Crystal and Nanodiamonds in Aqueous Lubrication. Film Thickness and Influence of Sliding Speed. *Wear* **2019**, *418*, 241–252. [[CrossRef](#)]
34. Hao, L.; Hao, W.; Li, P.; Liu, G.; Li, H.; Aljabri, A.; Xie, Z. Friction and Wear Properties of a Nanoscale Ionic Liquid-like GO@SiO₂ Hybrid as a Water-Based Lubricant Additive. *Lubricants* **2022**, *10*, 125. [[CrossRef](#)]
35. Lin, W.; Klein, J. Control of Surface Forces through Hydrated Boundary Layers. *Curr. Opin. Colloid Interface Sci.* **2019**, *44*, 94–106. [[CrossRef](#)]
36. Kreivaitis, R.; Gumbytė, M.; Kupčinskas, A.; Treinytė, J.; Sendžikienė, E. Synthesis and Tribological Properties of Bis(2-Hydroxyethyl)Ammonium Erucate as a Potential Environmentally Friendly Lubricant and Lubricant Additive. *Appl. Sci.* **2023**, *13*, 3401. [[CrossRef](#)]
37. Noor El-Din, M.R.; Mishrif, M.R.; Kailas, S.V.; Ps, S.; Mannekote, J.K. Studying the Lubricity of New Eco-Friendly Cutting Oil Formulation in Metal Working Fluid. *Ind. Lubr. Tribol.* **2018**, *70*, 1569–1579. [[CrossRef](#)]
38. Kim, K.T.; Kim, H.W.; Chang, H.Y.; Lim, B.T.; Park, H.B.; Kim, Y.S. Corrosion Inhibiting Mechanism of Nitrite Ion on the Passivation of Carbon Steel and Ductile Cast Iron for Nuclear Power Plants. *Adv. Mater. Sci. Eng.* **2015**, *2015*, 408138. [[CrossRef](#)]
39. Zheng, G.; Zhang, G.; Ding, T.; Xiang, X.; Li, F.; Ren, T.; Liu, S.; Zheng, L. Tribological Properties and Surface Interaction of Novel Water-Soluble Ionic Liquid in Water-Glycol. *Tribol. Int.* **2017**, *116*, 440–448. [[CrossRef](#)]
40. Stachowiak, G.W.; Batchelor, A.W. *Engineering Tribology*, 4th ed.; Butterworth-Heinemann: Oxford, UK, 2013.
41. Li, L.; Bai, P.; Wen, X.; Zhou, X.; Ma, K.; Meng, Y.; Ding, J.; Tian, Y. Wear Mechanism and Evolution of Tribofilm of Ceramic on Steel Pairs under Ester Oil Lubrication in Wide Temperature Range. *J. Mater. Res. Technol.* **2023**, *27*, 6984–6996. [[CrossRef](#)]
42. Peña-Parás, L.; Taha-Tijerina, J.; García, A.; Maldonado, D.; González, J.A.; Molina, D.; Palacios, E.; Cantú, P. Antiwear and Extreme Pressure Properties of Nanofluids for Industrial Applications. *Tribol. Trans.* **2014**, *57*, 1072–1076. [[CrossRef](#)]
43. Chang, H.; Lan, C.; Chen, C.; Kao, M.; Guo, J. Anti-Wear and Friction Properties of Nanoparticles as Additives in the Lithium Grease. *Int. J. Precis. Eng. Manuf.* **2014**, *15*, 2059–2063. [[CrossRef](#)]
44. Song, Z.; Liang, Y.; Fan, M.; Zhou, F.; Liu, W. Ionic Liquids from Amino Acids: Fully Green Fluid Lubricants for Various Surface Contacts. *RSC Adv.* **2014**, *4*, 19396–19402. [[CrossRef](#)]
45. Furey, M.J.; Kajdas, C.; Kempinski, R. Applications of the Concept of Tribopolymerisation in Fuels, Lubricants, Metalworking, and “minimalist” Lubrication. *Lubr. Sci.* **2002**, *15*, 73–82. [[CrossRef](#)]
46. Wang, Q.J.; Chung, Y.-W. *Encyclopedia of Tribology*; Springer: New York, NY, USA, 2013.
47. Xia, W.; Zhao, J.; Wu, H.; Zhao, X.; Zhang, X.; Xu, J.; Jiao, S.; Wang, X.; Zhou, C.; Jiang, Z. Effects of Oil-in-Water Based Nanolubricant Containing TiO₂ Nanoparticles in Hot Rolling of 304 Stainless Steel. *J. Mater. Process. Technol.* **2018**, *262*, 149–156. [[CrossRef](#)]

Disclaimer/Publisher’s Note: The statements, opinions and data contained in all publications are solely those of the individual author(s) and contributor(s) and not of MDPI and/or the editor(s). MDPI and/or the editor(s) disclaim responsibility for any injury to people or property resulting from any ideas, methods, instructions or products referred to in the content.